The Journal of Immunology

Targeting of Antigen to Dendritic Cells with Poly(γ-Glutamic Acid) Nanoparticles Induces Antigen-Specific Humoral and Cellular Immunity

Tomofumi Uto, Xin Wang, Katsuaki Sato, Misako Haraguchi, Takami Akagi, Mitsuru Akashi and Masanori Baba

J Immunol 2007; 178:2979-2986; ;
doi: 10.4049/jimmunol.178.5.2979
http://www.jimmunol.org/content/178/5/2979

The Journal of Immunology is published twice each month by
The American Association of Immunologists, Inc.,
1451 Rockville Pike, Suite 650, Rockville, MD 20852

Print ISSN: 0022-1767 Online ISSN: 1550-6606.

Targeting of Antigen to Dendritic Cells with Poly(γ-Glutamic Acid) Nanoparticles Induces Antigen-Specific Humoral and Cellular Immunity[1]

Tomofumi Uto,*¶ Xin Wang,*¶ Katsuaki Sato,† Misako Haraguchi,‡ Takami Akagi,§¶ Mitsuru Akashi,§¶ and Masanori Baba[2]*¶

Nanoparticles are considered to be efficient tools for inducing potent immune responses by an Ag carrier. In this study, we examined the effect of Ag-carrying biodegradable poly(γ-glutamic acid) (γ-PGA) nanoparticles (NPs) on the induction of immune responses in mice. The NPs were efficiently taken up by dendritic cells (DCs) and subsequently localized in the lysosomal compartments. γ-PGA NPs strongly induced cytokine production, up-regulation of costimulatory molecules, and the enhancement of T cell stimulatory capacity in DCs. These maturational changes of DCs involved the MyD88-mediated NF-κB signaling pathway. In vivo, γ-PGA NPs were preferentially internalized by APCs (DCs and macrophages) and induced the production of IL-12p40 and IL-6. The immunization of mice with OVA-carrying NPs induced Ag-specific CTL activity and Ag-specific production of IFN-γ in splenocytes as well as potent production of Ag-specific IgG1 and IgG2a Abs in serum. Furthermore, immunization with NPs carrying a $CD8^+$ T cell epitope peptide of *Listeria monocytogenes* significantly protected the infected mice from death. These results suggest that Ag-carrying γ-PGA NPs are capable of inducing strong cellular and humoral immune responses and might be potentially useful as effective vaccine adjuvants for the therapy of infectious diseases. *The Journal of Immunology,* **2007, 178: 2979–2986.**

The generation of robust and specific immune responses against infectious diseases is a primary goal of vaccination. Novel vaccine candidates being developed are capable of inducing both cellular and humoral immune responses (1, 2). For instance, vaccines against intracellular pathogens such as HIV type 1 and malaria are required to induce strong cellular immune responses, whereas vaccines targeting extracellular microorganisms have to induce humoral immune responses (3–7).

Almost 70 years ago, Freund and colleagues developed the highly potent adjuvant CFA, which is an emulsion of water and mineral oil containing killed mycobacteria (8). Despite a potent activity, CFA also induces severe local reactions and thus cannot be used for humans. Therefore, it seems mandatory to develop less toxic and more effective vaccine adjuvants. Aluminum-based compounds such as aluminum phosphate or hydroxide are safe and currently used as predominant adjuvants in humans. These compounds are able to induce Th2 responses, yet they have little capacity to stimulate Th1 immune responses (9).

Dendritic cells (DCs),[3] the most potent APCs, are defined by their dendritic morphology and unique phenotype. DCs consist of heterogeneous subsets with myeloid or lymphoid lineage as well as different levels of maturity in both lymphoid and peripheral tissues (10). Immature DCs (iDCs) sense the presence of invading pathogens via various pattern-recognition receptors and process the intracellular pathogens in inflammatory tissues. iDCs develop into mature DCs (mDCs) with the up-regulation of MHC and costimulatory molecules in inflammatory microenvironments (10–14). Subsequently, mDCs migrate to secondary lymphoid tissues where they present the processed Ags to naive T cells to effectively generate effector T cells (10). Therefore, the targeting of Ags to DCs is believed to be a promising strategy for the potent and efficient induction of Ag-specific protective immune responses (15–17).

Nanoparticles (NPs) are considered to be efficient Ag carriers and are widely investigated for their biological potential (18, 19). We have previously reported that Con A-immobilized polystyrene NPs could efficiently capture HIV-1 particles and gp120 Ags (20). Immunization with inactivated HIV-1-capturing NPs induced HIV-1-specific IgA Abs in the genital tract of mice (21, 22). Furthermore, intranasal immunization of mice with simian/HIV-capturing NPs could induce mucosal immune responses in macaques, and the macaques immunized with simian/HIV-NPs exhibited partial protection against vaginal and systemic challenge with the virus (23). However, because polystyrene is not biodegradable, it may not be applicable to the clinical situation as a vaccine material

*Division of Antiviral Chemotherapy, Center for Chronic Viral Diseases, Graduate School of Medical and Dental Sciences, Kagoshima University, Kagoshima, Japan; †Laboratory for Dendritic Cell Immunology, Research Center for Allergy and Immunology, Institute of Physical and Chemical Research (Japan), Yokohama Institute, Kanagawa, Japan; ‡Department of Biochemistry and Molecular Biology, Graduate School of Medical and Dental Sciences, Kagoshima University, Kagoshima, Japan; §Department of Molecular Chemistry, Graduate School of Engineering, Osaka University, Osaka, Japan; ¶Core Research for Evolutional Science and Technology (CREST), the Japan Science and Technology Agency (JST), Tokyo, Japan

Received for publication September 8, 2006. Accepted for publication December 22, 2006.

The costs of publication of this article were defrayed in part by the payment of page charges. This article must therefore be hereby marked *advertisement* in accordance with 18 U.S.C. Section 1734 solely to indicate this fact.

[1] This work was supported by Core Research for Evolutional Science and Technology from the Japan Science and Technology Agency.

[2] Address correspondence and reprint requests to Dr. Masanori Baba, Division of Antiviral Chemotherapy, Center for Chronic Viral Diseases, Graduate School of Medical and Dental Sciences, Kagoshima University, 8-35-1 Sakuragaoka, Kagoshima, Japan. E-mail address: m-baba@vanilla.ocn.ne.jp

[3] Abbreviations used in this paper: DC, dendritic cell; FITC-NP, FITC-labeled γ-PGA NP; FITC-OVA, FITC-conjugated OVA; FITC-OVA-NP, FITC-OVA-encapsulating NP; iDC, immature DC; LLO, listerolysin; mDC, mature DC; NP, nanoparticle; OVA-NP, OVA-carrying NP; γ-PGA, poly(γ-glutamic acid).

due to safety reasons. To improve the NP-based vaccine formation, we have successfully generated biodegradable NPs using poly(γ-glutamic acid) (γ-PGA) (24). γ-PGA is a capsular exopolymer produced by certain strains of bacteria. γ-PGA NPs are degraded by γ-glutamyl transpeptidase, which is widely distributed in the whole body. In addition, various molecules such as proteins and peptides can be immobilized on the surface and/or the inside of the particles. In this study, we examined the effect of γ-PGA NPs on DC functions and the efficacy of Ag-carrying γ-PGA NPs for the induction of Ag-specific immune responses.

Materials and Methods

Mice

Female C57BL/6 (H-2K^b, 6–8 wk of age) mice were purchased from Charles River. Experiments were approved by Kagoshima University and conducted in accordance with its guideline for animal experimentation.

Cells

B cells were obtained by the positive selection of splenic mononuclear cells from normal C57BL/6 mice using mAbs to B-220 (BD Biosciences) and sheep anti-rat IgG Ab-conjugated immunomagnetic beads (Dynal Biotech). Macrophages were obtained from peritoneal exudates in C57BL/6 mice injected with 100 μl of 1% thioglycolate. iDCs were prepared by culturing murine bone marrow cells in the presence of 20 ng/ml GM-CSF (PeproTech) for 7 days (25–27). mDCs were obtained from iDCs by cultivation with 1 μg/ml LPS (Sigma-Aldrich) for 2 days.

Nanoparticles

The synthetic procedures for γ-PGA NPs and OVA-carrying γ-PGA NPs (OVA-NPs) have been described in our previous report (28). FITC-labeled γ-PGA NPs (FITC-NPs) were synthesized as follows. γ-PGA was conjugated with L-phenylalanine ethylester and 5-aminoacetamido FITC (Molecular Probes) in the presence of water-soluble carbodiimide. The amount of incorporated FITC was measured by spectrofluorometer. γ-PGA NPs either immobilize or encapsulate the K^b-restricted CD8$^+$ T cell epitope listerolysin (LLO) peptide 296–307 (VAYGRQVYLKLS). LLO-immobilizing NPs were synthesized as follows. A carboxyl group of γ-PGA NPs (10 mg/ml) was activated by water-soluble carbodiimide (1 mg/ml in 20 mM phosphate buffer (pH 5.8)) for 20 min. The activated NPs (5 mg), collected by centrifugation (14,000 × *g* for 15 min), were mixed with 1 ml of the peptide (0.25 mg/ml) in PBS, and the mixture was incubated at 4°C for 24 h. After the reaction, the NPs were centrifuged, washed twice with water, and resuspended at 10 mg/ml in PBS. The amount of peptide was measured by the Lowry method, in which LLO-immobilizing or -encapsulating NPs were added to the same volume of 4% SDS to dissolve the γ-PGA NPs, and the peptide content was determined. One milligram of γ-PGA NPs contained 200 μg of the peptide. The contamination of bacterial endotoxin in γ-PGA NPs was determined by a *Limulus* amoebocyte lysate assay (Seikagaku) and found to be <10 endotoxin units/ml.

Uptake of γ-PGA NPs by APCs in vitro

B cells, macrophages, and iDCs (5 × 10^5 cells per 500 μl) were incubated with 100 μg/ml FITC-NPs for 30 min at 37°C and washed with PBS. The cell-associated fluorescence was measured by FACS (FACSCalibur; BD Biosciences). Cytometric data were analyzed by CellQuestPro (BD Biosciences). To determine intracellular NPs, iDCs were incubated with 10 μg/ml FITC-NPs for 30 min at 37°C and washed with PBS. The cell membrane was labeled with PE-conjugated anti-CD11c for 30 min on ice. The cells were washed twice with PBS and transferred to a 24-well glass-bottom culture plate (Asahi Techno Glass). The cells were fixed with 4% paraformaldehyde in PBS for 10 min at room temperature, washed twice with PBS, and subjected to analysis for intracellular localization of NPs by confocal laser scanning microscopy (LSM5 Pascal; Carl Zeiss). To analyze the intracellular localization of NPs, the lysosomes of iDCs were visualized with 50 nM LysoTracker Red DND-99 (Molecular Probes) for 30 min at 37°C. After washing, the cells were incubated with 10 μg/ml FITC-NPs for 30 min at 37°C. The cells were washed, fixed, and examined by confocal laser scanning microscopy as described above. To investigate the dose and time dependency of NP uptake by iDCs, the cells were incubated in the presence of various concentrations of FITC-NPs (1.5–100 μg/ml) at 37°C. The uptake of FITC-NPs at a fixed concentration (100 μg/ml) was examined at different incubation periods. After washing the cells, the cell-associated fluorescence was measured by FACS. To determine the uptake of FITC-conjugated OVA (FITC-OVA) or FITC-OVA-encapsulating NPs (FITC-OVA-NPs) by iDCs, the cells were incubated with FITC-OVA (25, 50, and 100 μg/ml) or FITC-OVA-NPs (carrying 25, 50, and 100 μg/ml FITC-OVA) for 30 min at 37°C. After washing the cells, the cell-associated fluorescence was measured by FACS.

Analysis for DC activation

To determine cytokine production, iDC (2.5 × 10^5 cells/ml) were stimulated with various concentrations of γ-PGA NPs or 1 μg/ml LPS. At 2, 6, 24, and 48 h after stimulation, culture supernatants were collected and measured for their IL-12p40 and TNF-α levels by ELISA kits (BioSource International). For phenotypic analysis, iDCs were stimulated with various concentrations of γ-PGA NPs or LPS for 48 h. The cells were washed with PBS, stained with a PE-conjugated anti-CD40 mAb (BD Biosciences) for 30 min at 4°C, and subjected to FACS analysis.

Allogeneic MLR

iDCs were stimulated with various concentrations of γ-PGA NPs, CpG oligodeoxynucleotides (InvivoGen), polyinosinic-polycytidylic acid (InvivoGen), or LPS for 48 h. The cells were collected and washed with PBS. T cells were obtained by the negative selection of splenic mononuclear cells obtained from normal BALB/c mice using mAbs to Ly-76, B-220, Ly-6G, and I-A/I-E (BD Biosciences) and sheep anti-rat IgG Ab-conjugated immunomagnetic beads. T cells and DCs were incubated at a ratio of 10:1 in a flat-bottom 96-well plate. After a 4-day incubation, 1 μCi (0.037 MBq) of [^{3}H]thymidine was added to each well. The cells were harvested after 16 h and examined for their radioactivity by liquid scintillation spectroscopy.

Analysis of activation signaling pathway

iDCs (2.5 × 10^5 cells/ml) were preincubated with various concentrations of either the p38 MAPK inhibitor SC68376, the JNK inhibitor SP600125, an ERK inhibitor peptide, or the NF-κB inhibitor parthenolide for 1 h (all from Calbiochem) (29–31). The cells were also preincubated with a MyD88 inhibitor peptide (IMGENEX) for 24 h (32). After incubation, the cells were stimulated with 300 μg/ml γ-PGA NPs or 1 μg/ml LPS for 16 h. Culture supernatants were collected for the determination of their TNF-α levels with an ELISA kit (BioSource International). For NF-κB activation analysis, iDCs (1.25 × 10^5 cells/ml) were stimulated with 300 μg/ml γ-PGA NPs or 1 μg/ml LPS for 2 h. The cells were fixed with 3.7% paraformaldehyde and permeabilized with 0.2% Triton X-100 for 5 min. Then, the cells were stained with a rabbit anti-NF-κB p65 polyclonal Ab for 60 min followed by a FITC-conjugated goat anti-rabbit IgG Ab (both from Santa Cruz Biotechnology) for 60 min at room temperature and subjected to confocal laser scanning microscopy.

Uptake of γ-PGA NPs by APCs in vivo

To examine the uptake of γ-PGA NPs by APCs, including DCs in vivo, FITC-NPs (2.7 mg in 500 μl of PBS) or PBS alone were injected i.v. to mice. After 4 h, spleen cells were collected from the mice and stained with either PE-conjugated anti-CD3 (for T cells), B220 (for B cells), CD11c (for DCs), or F4/80 (for macrophages) mAb and an allophycocyanin-conjugated anti-CD8a (for CD8a$^+$CD11c$^+$ DCs) mAb (all from BD Biosciences) for 30 min at 4°C. The cells were analyzed by FACS. The maturation of spleen DCs was assessed by the following procedures. γ-PGA NPs (5 mg/ml in PBS) or PBS alone were injected i.p. to mice. Their spleens were collected at 20, 40, and 64 h after injection, dissociated into single-cell suspensions, and stained with PE-conjugated anti-CD11c mAb and either FITC-conjugated anti-CD40, anti-CD80, or anti-CD86 mAb. The cells were also analyzed by FACS. For the detection of cytokine production in vivo, γ-PGA NPs (5 mg/ml in PBS) or PBS alone was injected i.p. to mice. At 4 h after injection, the serum levels of IL-12p40 and IL-6 were measured by ELISA.

Immunization of mice with OVA-carrying γ-PGA-NPs

Mice (3–5 mice in each group) were immunized with either PBS, OVA alone (100 μg), CFA plus OVA (100 μg of OVA in CFA), or OVA-NPs (1 mg of NPs carrying 100 μg of OVA) by a rear footpad route on days 0 and 7. On day 14 after the final immunization, spleen cells were collected and cultured with 10 μg/ml K^b-restricted CTL epitope peptide 257–264 of OVA (OVA$_{257–264}$) and 10 U/ml murine rIL-2 (PeproTech) for 5 days. The cells were served as effector cells to examine their OVA-specific CTL activity. EL4 (H-2K^b) cells untreated and treated with the OVA$_{257–264}$ peptide for 16 h were used as the control and target cells, respectively. The cells were labeled with 100 μCi/ml $Na_2[^{51}Cr]O_4$, mixed with the effector

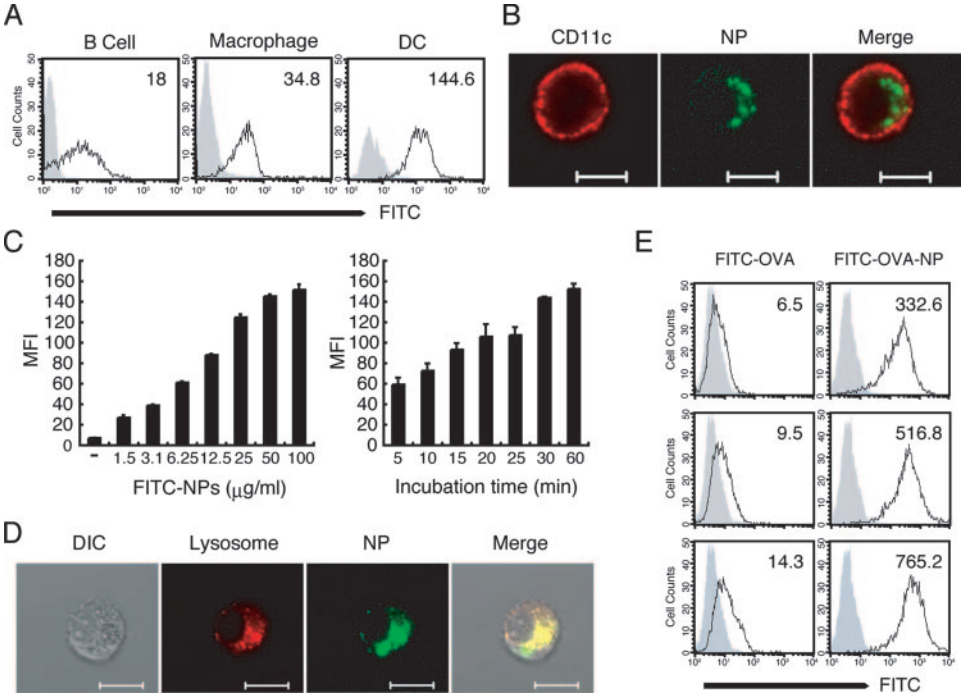

FIGURE 1. Uptake of FITC-γ-PGA NPs by iDCs in vitro. *A*, B cells, macrophages and iDCs were cultured in the presence of FITC-NPs for 30 min at 37°C and cell-associated fluorescence was assessed by flow cytometry. The number in each histogram indicates mean fluorescence intensity of the cells. *B*, iDCs were cultured in the presence of FITC-NPs (green) for 30 min at 37°C and then stained with a PE-conjugated anti-CD11c mAb (red) on ice. Intracellular localization of FITC-γ-PGA NPs was determined by confocal laser scanning microscopy. Bars indicate 10 μm. *C*, iDCs were cultured with the indicated concentrations of FITC-NPs for 60 min at 37°C or cultured with 100 μg/ml FITC-NPs for the indicated time periods at 37°C, and cell-associated fluorescence was assessed by flow cytometry. The experiment was performed in duplicate and results are expressed as mean fluorescence intensity (MFI) ± SD. The results are a representative of three separate experiments. *D*, iDCs were stained with LysoTracker Red DND-99 (red) and cultured in the presence of FITC-PGA NPs (green). Localization of lysosomes and FITC-NPs was determined by confocal laser scanning microscopy. Bars indicate 10 μm. DIC, differential interference contrast. *E*, iDCs were cultured in the presence of FITC-OVA or FITC-OVA-NPs for 30 min at 37°C, and cell-associated fluorescence was assessed by flow cytometry. FITC-OVA concentrations were 25, 50, and 100 μg/ml in *upper*, *middle*, and *lower panels*, respectively.

cells at various effector/target ratios, and further incubated for 4 h. Ag-specific lysis of the target cells was monitored by a standard ^{51}Cr-releasing method as previously described (26).

IFN-γ-producing cells were evaluated by ELISPOT with a mouse IFN-γ ELISPOT kit (BD Biosciences). The collected spleen cells (1×10^6 cells/ml) were restimulated with 10 μg/ml OVA or the $OVA_{257–264}$ peptide in a 96-well ELISPOT plate. The plate was incubated at 37°C for 18 h, washed, and further incubated with a biotin-conjugated detection Ab for 2 h at room temperature. After washing, the plate was incubated with streptavidin-conjugated HRP and incubated for 1 h. The plate was washed again and incubated with the substrate for 15 min. The colorimetric reaction was terminated by washing with water. After drying the plate, the number of spots was counted microscopically.

Serum samples were also collected from the mice on day 14 after the final immunization and subjected to measurement of their anti-OVA Ab titers by ELISA. Briefly, a 96-well plate was coated with OVA suspension in carbonate-bicarbonate buffer (10 μg/ml) and incubated overnight at 4°C. The plate was washed with PBS containing 0.05% Tween 20 (T-PBS) and incubated with 1% BSA and 1% skim milk in T-PBS for 2 h at room temperature. The serum samples serially diluted with T-PBS were added to the wells. After a 2-h incubation at room temperature, the plate was incubated with either alkaline phosphatase-conjugated goat anti-mouse IgG, IgG1, or IgG2a Ab (Southern Biotechnology). The plate was developed by adding the substrate to each well and incubated for 10 min. The colorimetric reaction was terminated by adding a stop solution (2M H_2SO_4), and the absorbance of each well was measured at 450 nm. End point titers were determined by the *x*-axis intercept of the dilution curve.

Listeria monocytogenes *challenge to immunized mice*

Eight mice in each group were immunized with either PBS, LLO peptide alone (100 μg), LLO-immobilizing NPs, or LLO-encapsulating NPs (1 mg of both NPs carrying 10 μg of the peptide) by a rear footpad route on days 0 and 7. On day 14 after the final immunization, the mice were challenged with 5×10^5 of virulent *L. monocytogenes*.

Statistical analysis

Statistical evaluation was performed by Student's *t* test. Statistical analysis for survival of mice was performed with the computer software StatView-J version 5.0.

Results

Uptake of γ-PGA NPs by APCs in vitro

When spleen B cells, peritoneal macrophages, and bone marrow-derived DCs were incubated with FITC-NPs and examined for their NP uptake by flow cytometry, DCs were found to take up FITC-NPs more efficiently than B cells and macrophages (Fig. 1*A*). To determine the intracellular localization γ-PGA NPs, DCs were incubated with FITC-NPs and then labeled with a PE-conjugated anti-CD11c mAb. Green signals inside of the cell membrane clearly showed the uptake of NPs by DCs (Fig. 1*B*). When the dose and time dependency of NP uptake by DCs was examined, the amount of intracellular NPs increased with increasing concentrations and incubation times of NPs, indicating that the uptake was both dose and time dependent (Fig. 1*C*). However, a further increase of incubation time up to 24 h did not significantly increase the amount of intracellular NPs (data not shown). To further determine the intracellular localization of NPs in DCs, lysosomes were stained with a lysosome-specific dye. Internalized NPs were mostly detected along with the lysosomes of DCs (Fig. 1*D*),

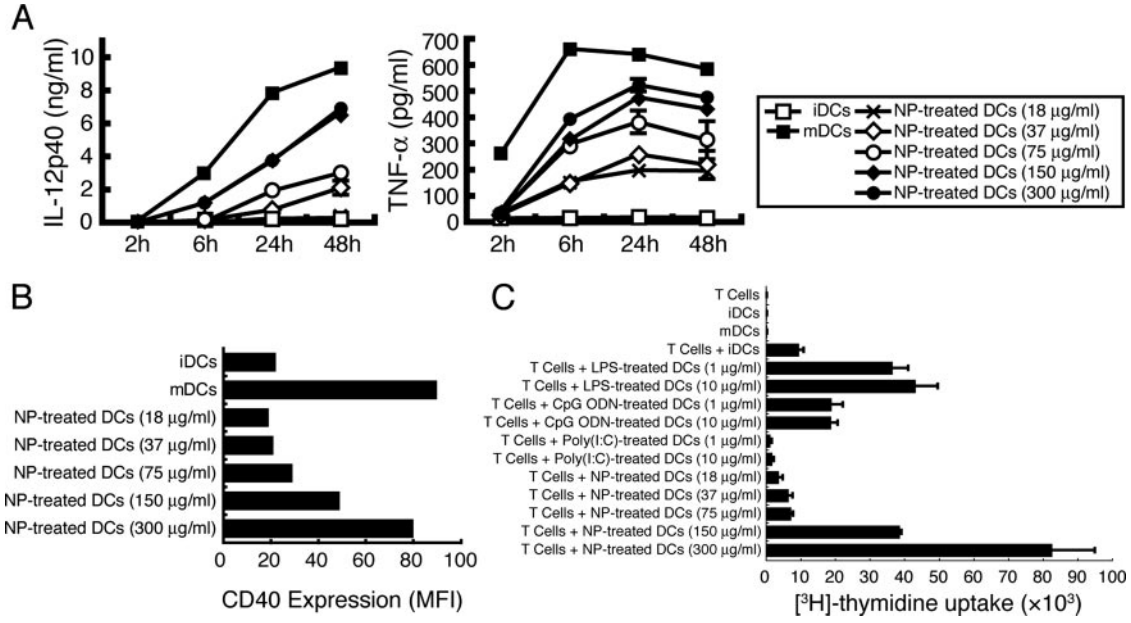

FIGURE 2. Maturation and activation of DCs by γ-PGA NPs. *A*, iDCs were cultured with the indicated concentrations of γ-PGA NPs or 1 μg/ml LPS. Culture supernatants were collected at different time points after cultivation. Cytokine levels were measured by ELISA. The experiment was performed in duplicate, and the results are expressed as means ± ranges. The results are a representative of three separate experiments. *B*, iDCs were cultured in the presence of indicated concentration of γ-PGA NPs or 1 μg/ml LPS. After 2 days the cells were collected, stained with anti-CD11c-PE and anti-CD40-FITC mAbs, and analyzed by flow cytometry. Data are expressed as mean fluorescence intensity (MFI). The results are a representative of three separate experiments. *C*, iDCs were cultured with the indicated concentrations of γ-PGA NPs, CpG oligodeoxynucleotide (ODN), polyinosinic-polycytidylic acid (poly(I:C)), or LPS. After 2 days the cells were collected and cocultured with allogeneic normal T cells for 4 days. Proliferative response was measured by [^{3}H]thymidine uptake on day 5. Data are expressed as mean ± SD. The results are a representative of three separate experiments.

indicating that internalized NPs preferentially localized in the lysosomal compartments. Furthermore, it is clear that the NP-associated form of OVA (FITC-OVA-NPs) could be taken up much more efficiently by DCs than the NP-free form of OVA (FITC-OVA) (Fig. 1*E*). γ-PGA NPs did not affect the viability of DCs after 48 h of cocultivation at concentrations up to 300 μg/ml (data not shown).

Maturation and activation of DCs by γ-PGA NPs

To examine the effect of γ-PGA NPs on DC maturation, iDCs were cultured in the presence of various concentrations of γ-PGA NPs. When cytokine production was examined, iDCs did not produce detectable levels of IL-12p40 and TNF-α. In contrast, both cytokines were abundantly produced from mDCs and NP-treated DCs in dose- and time-dependent fashions (Fig. 2*A*). Furthermore, NP-treated DCs also produced IL-1β and IL-6 (data not shown). The maturation of iDCs is accompanied by the enhanced expression of surface markers, including costimulatory molecules and MHC complexes. Treatment of iDCs with γ-PGA NPs resulted in a marked increase of CD40 expression on their surfaces in a dose-dependent fashion (Fig. 2*B*). CD86, MHC class I, and MHC class II expressions were also up-regulated in NP-exposed DCs, as compared with iDCs (data not shown). Like mDCs, NP-treated DCs showed strong capacity to stimulate allogeneic T cells in a dose-dependent fashion (Fig. 2*C*).

γ-PGA NPs induce NF-κB activation via a MyD88-dependent pathway

To clarify the signaling pathway underlying γ-PGA NP-induced DC maturation, we examined the effect of various inhibitors on γ-PGA NP-induced TNF-α production in DCs. Treatment with the p38 MAPK inhibitor SC68376 suppressed both LPS- and NP-induced TNF-α production, whereas the JNK inhibitor SP600125 failed to do so (Fig. 3*A*). Although an ERK inhibitor peptide did not inhibit NP-induced TNF-α production, it suppressed LPS-induced TNF-α production (Fig. 3*A*). In contrast, a MyD88 inhibitor peptide, but not a control peptide, significantly reduced TNF-α production in both NP- and LPS-treated DCs (Fig. 3*B*). We also examined the nuclear translocation of the p65 subunit of NF-κB by confocal laser scanning microscopy. The p65 subunit was located in the cytoplasm of the untreated cells, whereas the translocation of p65 into the nucleus was detected in both NP- and LPS-treated DCs (Fig. 3*C*). Furthermore, treatment with the NF-κB inhibitor parthenolide showed more profound suppression on TNF-α production in NP-treated DCs than in LPS-treated DCs (Fig. 3*D*).

Uptake of γ-PGA NPs by APCs in vivo

To examine the uptake of γ-PGA NPs in vivo, spleen cells were collected from mice at 4 h after i.v. administration of FITC-NPs. The FITC-positive cells were detectable in B cells, DCs, and macrophages but not in T cells. The number of FTIC-positive cells was the highest in DCs compared with other cell types (Fig. 4*A*). CD8a$^+$ lymphoid DCs play an important role in the initiation of the Th1 cell-biased immune response as well as the cross-presentation of processed Ags to CD8$^+$ T cells, leading to the generation of Ag-specific CTLs (17). To determine whether FITC-NPs are taken up by CD8a$^+$ DCs, the spleen cells were stained with anti-CD11c and anti-CD8 mAbs and examined for their FITC-positive population. Approximately one-third (34.3%) of the FITC-positive cells were CD11c$^+$ DCs, and 3.21% of the FITC-positive cells (9.4% of the CD11c$^+$ DCs) was also CD8a$^+$ (Fig. 4*B*). When CD40, CD80, and CD86 expressions were examined

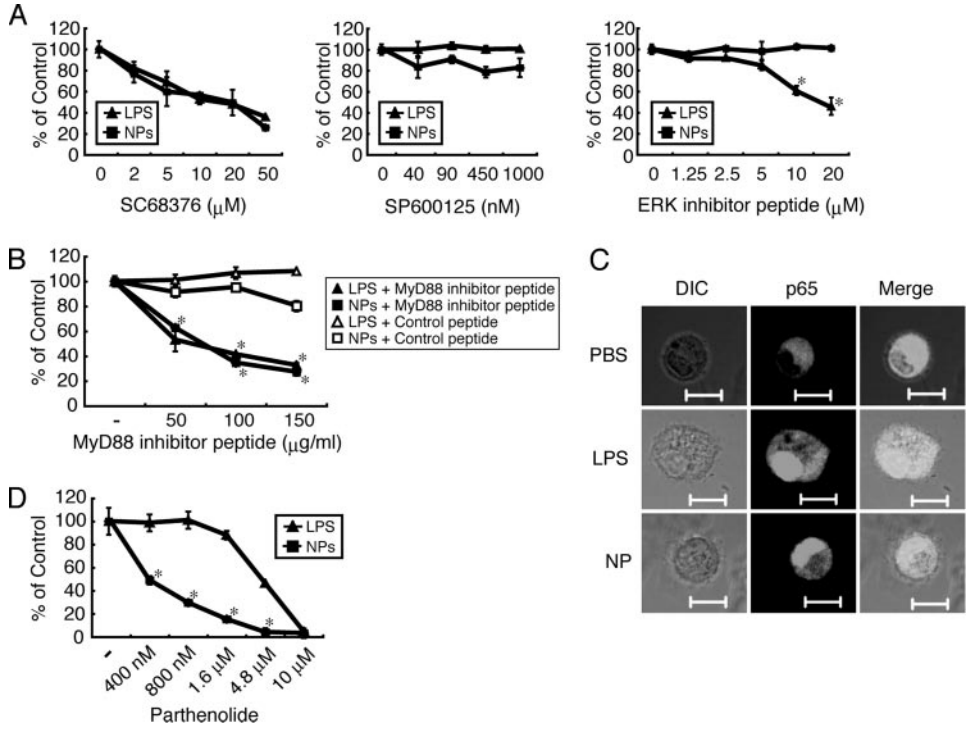

FIGURE 3. Effect of various inhibitors on DC activation by γ-PGA NPs. *A*, iDCs were preincubated with the indicated concentrations of SC68376, SP600125, or an ERK inhibitor peptide for 1 h. After incubation, the cells were stimulated with 300 μg/ml γ-PGA NPs or 1 μg/ml LPS and cultured for 16 h. Culture supernatants were collected and determined for their TNF-α level by ELISA. *B*, iDCs were preincubated with the indicated concentrations of either a MyD88 inhibitor peptide or a control peptide for 1 h. After incubation, the cells were stimulated with 300 μg/ml γ-PGA NPs or 1 μg/ml LPS and cultured for 16 h. Culture supernatants were collected and determined for their TNF-α level by ELISA. *C*, iDCs were stimulated with 300 μg/ml γ-PGA or 1 μg/ml LPS for 2 h. The cells were fixed, permeabilized, and stained with a rabbit anti-NF-κB p65 polyclonal Ab followed by an FITC-conjugated goat anti-rabbit IgG Ab. The localization of p65 was determined by confocal laser scanning microscopy. Bars indicate 10 μm. *D*, iDCs were preincubated with the indicated concentrations of parthenolide. After incubation, the cells were stimulated with 300 μg/ml γ-PGA NPs or 1 μg/ml LPS and cultured for 16 h. Culture supernatants were collected to determine their TNF-α level. Except for the p65 localization experiment, all experiments were performed in triplicate and data are expressed as means ± SD. The results are a representative of three separate experiments. Statistical evaluation for the results was conducted between the corresponding two groups. *, $p < 0.05$.

for spleen DCs obtained from NP-treated mice, the enhanced expression of these molecules was identified most clearly at 40 h after NP-treatment of mice (Fig. 4*C*). However, such enhancement was not observed for PBS-treated mice. The serum IL-12p40 and IL-6 levels were found to be significantly higher in NP-treated mice than in PBS-treated mice (Fig. 4*D*).

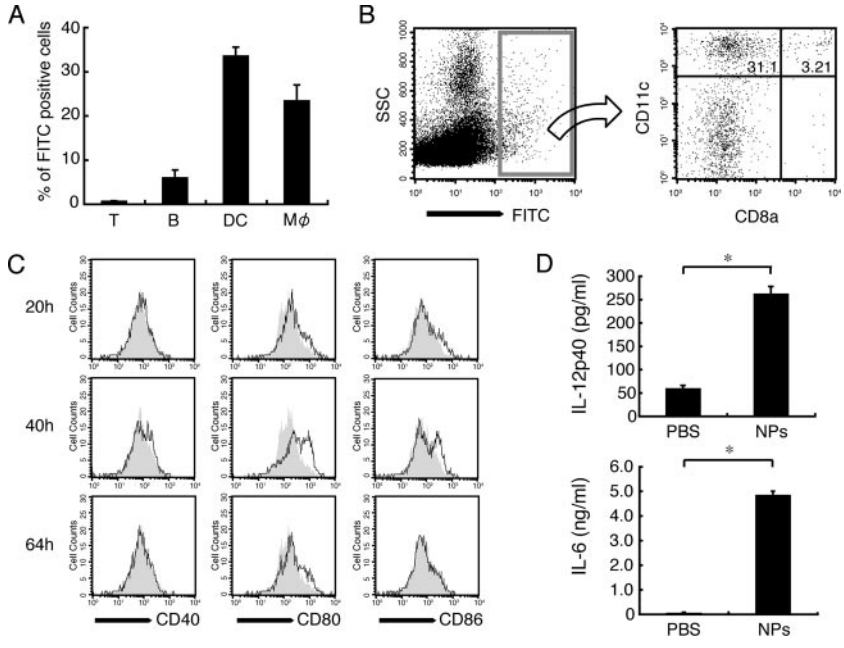

FIGURE 4. Uptake of γ-PGA NPs by DCs and their maturation in vivo. *A*, PBS or 2.7 mg of FITC-NPs were injected into mice through their tail veins. After 4 h, spleen cells (T, T cells; B, B cells; Mϕ, macrophages) were collected, stained with PE-conjugated anti-CD3, anti-B220, anti-CD11c, or anti-F4/80 mAbs, and analyzed by flow cytometry. *B*, PBS or FITC-NPs were injected, as described above. Spleen cells were collected and stained with PE-conjugated anti-CD11c and allophycocyanin-conjugated anti-CD8a mAbs. The FITC-positive cells were analyzed by FACS. The results from a representative experiment among three separate experiments are shown. *C*, PBS or 5 mg of γ-PGA NPs were injected i.p. to mice. At various time points spleen cells were collected, stained with PE-conjugated anti-CD11c and FITC-conjugated anti-CD40, anti-CD80, and anti-CD86 mAbs, and analyzed by flow cytometry. *D*, PBS or 5 mg of γ-PGA NPs were injected i.p. to mice. After 4 h, sera were collected and cytokine levels were measured by ELISA. The experiment was performed in triplicate, and data are expressed as means ± SD. *, $p < 0.05$.

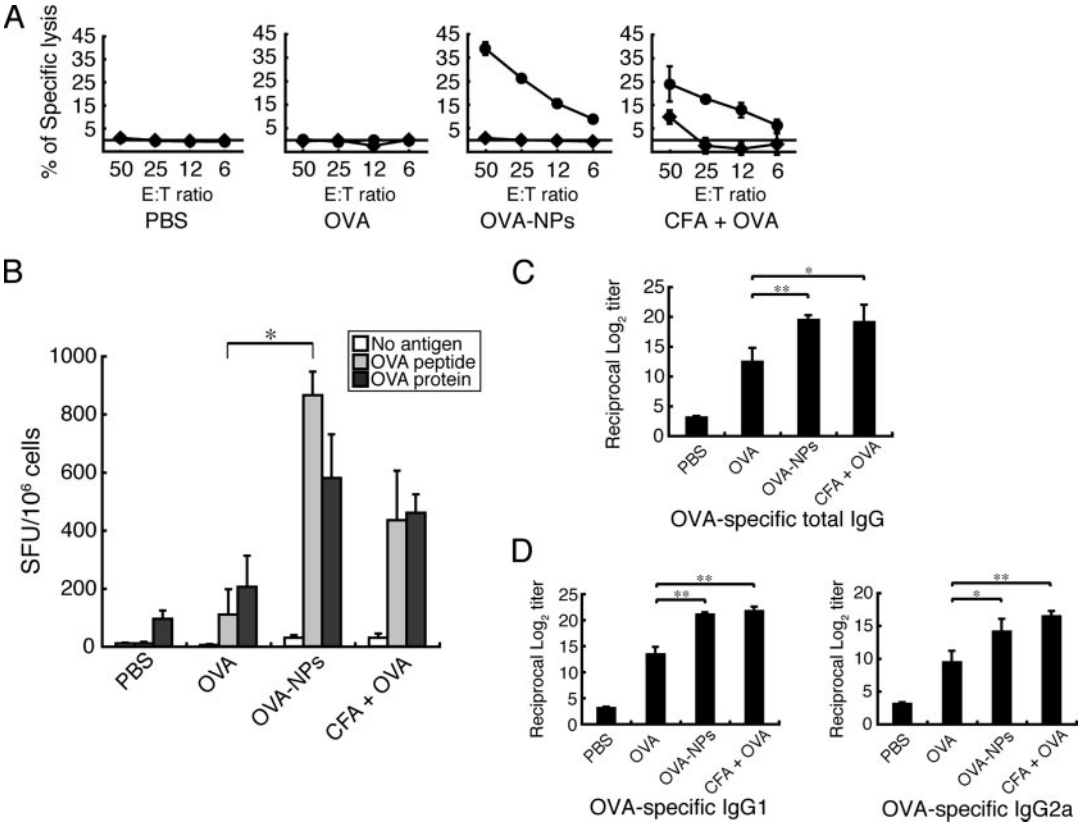

FIGURE 5. Induction of Ag-specific cellular and humoral immune responses by OVA-NPs. Mice were immunized with either PBS, OVA, OVA-NPs, or CFA plus OVA through their footpads. *A*, Spleen cells were restimulated with the $OVA_{257–264}$ peptide and IL-2. The spleen cells were examined for their cytolytic activity to peptide-treated or untreated EL4 target cells at various E:T ratios by a standard ^{51}Cr-releasing assay. The experiments were performed in triplicate, and data are expressed as means ± SD. The results are a representative of three separate experiments. The difference in specific lysis between the OVA-NPs group and the CFA plus OVA group is statistically significant ($p < 0.05$) at an E:T ratio of 50. *B*, Spleen cells were restimulated with the $OVA_{257–264}$ peptide or OVA protein. IFN-γ producing T cells were counted and expressed as the spot forming unit (SFU) per one million cells. Data represent means ± SD for three to four separate experiments. ∗, $p < 0.05$. *C* and *D*, Sera were tested for their Ab titers of OVA-specific IgG and its subclasses as determined by ELISA. Data represent means ± SD of endpoint titers for three to four separate experiments. ∗, $p < 0.05$, ∗∗, $p < 0.005$.

OVA-carrying γ-PGA NPs induce Ag-specific immune responses

The efficacy of Ag-capturing γ-PGA NPs on the induction of Ag-specific cellular and humoral immune responses was examined using OVA as a model Ag. As shown in Fig. 5*A*, an Ag-specific CTL response was not observed in the spleen cells obtained from the control (PBS) and OVA-immunized mice. In contrast, the spleen cells obtained from the mice immunized with OVA-NPs showed a more potent Ag-specific CTL response than those obtained from mice immunized with OVA plus CFA (Fig. 5*A*). In addition, the number of Ag-specific IFN-γ producing cells was significantly higher in the OVA-NP group than the OVA group (Fig. 5*B*). When a K^b-restricted control peptide was used for stimulation, no such induction of IFN-γ producing cells was identified (data not shown). Furthermore, a similar level of cellular immune responses was observed in mice immunized with reduced doses of OVA-NPs (data not shown). When Ag-specific Ab responses were examined and compared among the groups after immunization, both OVA-NP- and (OVA plus CFA)-immunized mice showed significantly higher levels of OVA-specific total IgG, IgG1, and IgG2a Abs than OVA-immunized mice (Fig. 5, *C* and *D*).

Protection of mice from L. monocytogenes *infection*

Challenge with a lethal dose of live bacteria is a stringent test for the efficacy of vaccination. *L. monocytogenes* infection in mice seems to be a representative model for evaluating $CD8^+$ T cell-mediated protection against intracellular pathogens (33–35). Fourteen days after the final immunization the mice were infected with a lethal dose of viable *L. monocytogenes* and monitored daily for their survival. Approximately 80% of the mice immunized with

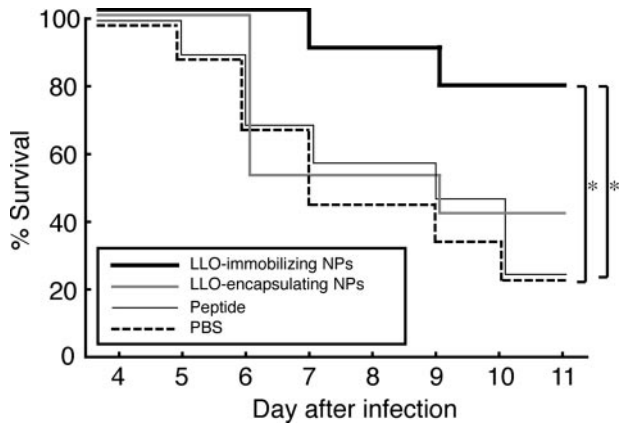

FIGURE 6. Protection of mice from *L. monocytogenes* infection. Mice (8 mice in each group) were immunized with either PBS (dotted line), LLO peptide alone (solid line), LLO-immobilizing NPs (heavy line), or LLO-encapsulating NPs (gray line) by a rear footpad route on days 0 and 7. On day 14 after the final immunization, the mice were infected with a lethal dose of *L. monocytogenes*. Survival of mice after infection was monitored up to 11 days. ∗, $p < 0.05$.

LLO-immobilizing NPs had survived by day 11 after infection. In contrast, most of the control mice and those immunized with the LLO peptide alone succumbed to the infection (Fig. 6). Little if any protection was observed for the mice immunized with LLO-encapsulating NPs. These results indicate that immunization with LLO-immobilizing NPs was efficient in protecting the mice from lethal infection with *L. monocytogenes*.

Discussion

Several attempts have been made to identify the strategies that induce potent immunostimulatory activities (36–38). However, most of the experimental adjuvants cannot be used for humans due to their side effects. At present, only the aluminum salt alum has been approved for clinical use, yet it has only weak activity. We have recently created biodegradable γ-PGA NPs that have potent immunomodulatory activities as well as an excellent capacity of carrying various proteins and peptides.

In this study, we showed that γ-PGA NPs were taken up by DCs most efficiently than by other APCs, such as macrophages and B cells, and localized in the lysosomes (Fig. 1). Although the mechanism of NP uptake remains to be elucidated, phagocytosis inhibitors showed modest (~30%) inhibition of the uptake by DCs (data not shown). It has been demonstrated that exogenous peptides can be acquired for cross-presentation to T cells through the MHC class I in the endolysosomal compartment of DCs (39). Analysis of the functional properties of DCs revealed that γ-PGA NPs were able to strongly induce DC activation. Activation of DCs through CD40 and IL-12p40 signaling pathways were needed for linkage between innate and adaptive immunity, including $CD4^+$ and $CD8^+$ T cell responses to DCs (40). In fact, NP-treated DCs could induce the production of the innate inflammatory cytokines IL-12p40 and TNF-α as well as CD40 expression and the strong stimulation of allogeneic T cells (Fig. 2). These results suggest that γ-PGA NPs are capable of inducing both innate and adaptive immunity through DC activation.

Analysis of the signaling pathway in NP-treated DCs indicated the involvement of MyD88-mediated NF-κB activation and p38 MAPK (Fig. 3). Similar results were also obtained with LPS-treated DCs. However, the ERK inhibitor could suppress TNF-α production in LPS-treated DCs but not in NP-treated DCs. Furthermore, the NF-κB inhibitor parthenolide was found to more effectively suppress TNF-α production in NP-treated DCs than in LPS-treated DCs. Thus, it appears that the signaling pathway involved in NP stimulation overlaps but is not identical with the pathway involved in LPS-stimulation. Presumably, fewer numbers of signal transduction molecules may participate in NP-induced NF-κB activation than in LPS-induced NF-κB activation. It is also noteworthy that unparticulated γ-PGA did not have sufficient activity to induce DC maturation (data not shown), indicating that the nanoparticle form of γ-PGA is required to interact with a certain molecule necessary for DC activation. Further studies are in progress to determine whether γ-PGA NPs interact with TLRs.

Because γ-PGA NPs proved to be predominantly taken up into spleen DCs and could up-regulate the expression of costimulatory molecules in vivo (Fig. 4), the γ-PGA NPs seem to be a promising candidate for a vaccine adjuvant. The uptake of Ags by DCs results in their subsequent migration to lymph nodes, increased production of cytokines, and enhanced expression of costimulatory and MHC molecules followed by Ag presentation to T cells. In mice DCs are divided into three subclasses, $CD11c^+CD8a^+CD4^-$, $CD11c^+CD8a^-CD4^-$, and $CD11c^+CD8a^-CD4^+$ (41). $CD8a^+$ DCs have been shown to play an important role in cross-priming to $CD8^+$ T cells (42, 43). Indeed, γ-PGA NPs were found to be taken up by $CD8a^+$ DCs, which may directly activate T cells in vivo.

OVA-NPs strongly induced OVA-specific IFN-γ producing cells, CTL activity, and Ab production (Fig. 5). These results suggest that potent cellular and humoral immune responses can be generated by γ-PGA NPs carrying not only OVA but also other peptides or proteins. In fact, γ-PGA NPs carrying HIV-1 Ags were found to induce strong Ag-specific cellular and humoral immunity in mice (X. Wang, T. Uto, T. Akagi, M. Akashi, and M. Baba, manuscript in preparation). Another remarkable observation is that LLO-immobilizing NPs could protect the immunized mice from lethal infection with the intracellular bacterium *L. monocytogenes* (Fig. 6). Taken together, γ-PGA NPs have great potential not only as efficient vaccine carriers but also as effective adjuvants in vivo.

In conclusion, the present study clearly shows the effectiveness of the γ-PGA NP as an Ag delivery system and an adjuvant to DCs in vitro and in vivo. Further studies, including the optimization of γ-PGA NPs and immunization with Ag-carrying NPs in other animal species, are in progress for the clinical development of this novel vaccine candidate.

Acknowledgment

We thank Dr. C. Koriyama for excellent advice on statistical evaluation in mouse experiments.

Disclosures

M. A. and M. B. are applying for a patent on nanoparticles. All other authors have no financial conflicts of interest.

References

1. Hutchings, C. L., S. C. Gilbert, A. V. Hill, and A. C. Moore. 2005. Novel protein and poxvirus-based vaccine combinations for simultaneous induction of humoral and cell-mediated immunity. *J. Immunol.* 175: 599–606.
2. Tritel, M., A. M. Stoddard, B. J. Flynn, P. A. Darrah, C. Y. Wu, U. Wille, J. A. Shah, Y. Huang, L. Xu, M. R. Betts, et al. 2003. Prime-boost vaccination with HIV-1 Gag protein and cytosine phosphate guanosine oligodeoxynucleotide, followed by adenovirus, induces sustained and robust humoral and cellular immune responses. *J. Immunol.* 171: 2538–2547.
3. Hanke, T., A. J. McMichael, M. Mwau, E. G. Wee, I. Ceberej, S. Patel, J. Sutton, M. Tomlinson, and R. V. Samuel. 1998. Development of a DNA-MVA/HIVA vaccine for Kenya. *Vaccine* 20: 1995–1998.
4. Moore, A. C., and A. V. Hill. 2004. Progress in DNA-based heterologous prime-boost immunization strategies for malaria. *Immunol. Rev.* 199: 126–143.
5. Schneider, J., S. C. Gilbert, T. J. Blanchard, T. Hanke, K. J. Robson, C. M. Hannan, M. Becker, R. Sinden, G. L. Smith, and A. V. Hill. 1998. Enhanced immunogenicity for $CD8^+$ T cell induction and complete protective efficacy of malaria DNA vaccination by boosting with modified vaccinia virus Ankara. *Nat. Med.* 4: 397–402.
6. Letvin, N. L., D. H. Barouch, and D. C. Montefiori. 2002. Prospects for vaccine protection against HIV-1 infection and AIDS. *Annu. Rev. Immunol.* 20: 73–99.
7. Good, M. F., D. C. Kaslow, and L. H. Miller. 1998. Pathways and strategies for developing a malaria blood-stage vaccine. *Annu. Rev. Immunol.* 16: 57–87.
8. Freund, J., J. Casals, and E. P. Hosmer. 1937. Sensitization and antibody formation after injection of tubercle bacili and paraffin oil. *Proc. Soc. Exp. Biol. Med.* 37: 509–513.
9. Petrovsky, N., and J. C. Aguilar. 2004. Vaccine adjuvants: current state and future trends. *Immunol. Cell Biol.* 82: 488–496.
10. Banchereau, J., F. Briere, C. Caux, J. Davoust, S. Lebecque, Y. J. Liu, B. Pulendran, and K. Palucka. 2000. Immunobiology of dendritic cells. *Annu. Rev. Immunol.* 18: 767–811.
11. Krieg, A. M. 2002. CpG motifs in bacterial DNA and their immune effects. *Annu. Rev. Immunol.* 20: 709–760.
12. Iwasaki, A., and R. Medzhitov. 2004. Toll-like receptor control of the adaptive immune responses. *Nat. Immunol.* 5: 987–995.
13. Sparwasser, T., E. S. Koch, R. M. Vabulas, K. Heeg, G. B. Lipford, J. W. Ellwart, and H. Wagner. 1998. Bacterial DNA and immunostimulatory CpG oligonucleotides trigger maturation and activation of murine dendritic cells. *Eur. J. Immunol.* 28: 2045–2054.
14. Lore, K., M. R. Betts, J. M. Brenchley, J. Kuruppu, S. Khojasteh, S. Perfetto, M. Roederer, R. A. Seder, and R. A. Koup. 2003. Toll-like receptor ligands modulate dendritic cells to augment cytomegalovirus- and HIV-1-specific T cell responses. *J. Immunol.* 171: 4320–4328.
15. Badovinac, V. P., K. A. Messingham, A. Jabbari, J. S. Haring, and J. T. Harty. 2005. Accelerated $CD8^+$ T-cell memory and prime-boost response after dendritic-cell vaccination. *Nat. Med.* 11: 748–756.

16. Luci, C., C. Hervouet, D. Rousseau, J. Holmgren, C. Czerkinsky, and F. Anjuere. 2006. Dendritic cell-mediated induction of mucosal cytotoxic responses following intravaginal immunization with the nontoxic B subunit of cholera toxin. *J. Immunol.* 176: 2749–2757.
17. Porgador, A., and E. Gilboa. 1995. Bone marrow-generated dendritic cells pulsed with a class I-restricted peptide are potent inducers of cytotoxic T lymphocytes. *J. Exp. Med.* 182: 255–260.
18. Coester, C., P. Nayyar, and J. Samuel. 2006. In vitro uptake of gelatin nanoparticles by murine dendritic cells and their intracellular localisation. *Eur. J. Pharm. Biopharm.* 62: 306–314.
19. Dinauer, N., S. Balthasar, C. Weber, J. Kreuter, K. Langer, and H. von Briesen. 2005. Selective targeting of antibody-conjugated nanoparticles to leukemic cells and primary T-lymphocytes. *Biomaterials* 26: 5898–5906.
20. Hayakawa, T., M. Kawamura, M. Okamoto, M. Baba, T. Niikawa, S. Takehara, T. Serizawa, and M. Akashi. 1998. Concanavalin A-immobilized polystyrene nanospheres capture HIV-1 virions and gp120: potential approach towards prevention of viral transmission. *J. Med. Virol.* 56: 327–331.
21. Kawamura, M., T. Naito, M. Ueno, T. Akagi, K. Hiraishi, I. Takai, M. Makino, T. Serizawa, K. Sugimura, M. Akashi, and M. Baba. 2002. Induction of mucosal IgA following intravaginal administration of inactivated HIV-1-capturing nanospheres in mice. *J. Med. Virol.* 66: 291–298.
22. Akagi, T., M. Kawamura, M. Ueno, K. Hiraishi, M. Adachi, T. Serizawa, M. Akashi, and M. Baba. 2003. Mucosal immunization with inactivated HIV-1-capturing nanospheres induces a significant HIV-1-specific vaginal antibody response in mice. *J. Med. Virol.* 69: 163–172.
23. Miyake, A., T. Akagi, Y. Enose, M. Ueno, M. Kawamura, R. Horiuchi, K. Hiraishi, M. Adachi, T. Serizawa, O. Narayan, et al. 2004. Induction of HIV-specific antibody response and protection against vaginal SHIV transmission by intranasal immunization with inactivated SHIV-capturing nanospheres in macaques. *J. Med. Virol.* 73: 368–377.
24. Akagi, T., M. Higashi, T. Keneko, T. Kida, and M. Akashi. 2005. In vitro enzymatic degradation of nanoparticles prepared from hydrophobically-modified poly(γ-glutamic acid). *Macromol. Biosci.* 14: 598–602.
25. Wang, X., T. Uto, K. Sato, K. Ide, T. Akagi, M. Okamoto, T. Kaneko, M. Akashi, and M. Baba. 2005. Potent activation of antigen-specific T cells by antigen-loaded nanospheres. *Immunol. Lett.* 98: 123–130.
26. Sato, K., N. Yamashita, N. Yamashita, M. Baba, and T. Matsuyama. 2003. Regulatory dendritic cells protect mice from murine acute graft-versus-host disease and leukemia relapse. *Immunity* 18: 367–379.
27. Sato, K., N. Yamashita, M. Baba, and T. Matsuyama. 2003. Modified myeloid dendritic cells act as regulatory dendritic cells to induce anergic and regulatory T cells. *Blood* 101: 3581–3589.
28. Akagi, T., T. Kaneko, T. Kida, and M. Akashi. 2005. Preparation and characterization of biodegradable nanoparticles based on poly(γ-glutamic acid) with l-phenylalanine as a protein carrier. *J. Controlled Release* 108: 226–236.
29. Bennett, B. L., D. T. Sasaki, B. W. Murray, E. C. O'Leary, S. T. Sakata, W. Xu, J. C. Leisten, A. Motiwala, S. Pierce, Y. Satoh, et al. 2001. SP600125, an anthrapyrazolone inhibitor of Jun N-terminal kinase. *Proc. Natl. Acad. Sci. USA* 98: 13681–13686.
30. Kelemen, B. R., K. Hsiao, and S. A. Goueli. 2002. Selective in vivo inhibition of mitogen-activated protein kinase activation using cell-permeable peptides. *J. Biol. Chem.* 277: 8741–8748.
31. Bork, P. M., M. L. Schmitz, M. Kuhnt, C. Escher, and M. Heinrich. 1997. Sesquiterpene lactone containing Mexican Indian medicinal plants and pure sesquiterpene lactones as potent inhibitors of transcription factor NF-κB. *FEBS Lett.* 402: 85–90.
32. Loiarro, M., C. Sette, G. Gallo, A. Ciacci, N. Fanto, D. Mastroianni, P. Carminati, and V. Ruggiero. 2005. Peptide-mediated interference of TIR domain dimerization in MyD88 inhibits interleukin-1-dependent activation of NF-κB. *J. Biol. Chem.* 280: 15809–15814.
33. Nagata, T., T. Aoshi, M. Suzuki, M. Uchijima, Y. H. Kim, Z. Yang, and Y. Koide. 2002. Induction of protective immunity to *Listeria monocytogenes* by immunization with plasmid DNA expressing a helper T-cell epitope that replaces the class II-associated invariant chain peptide of the invariant chain. *Infect. Immun.* 70: 2676–2680.
34. Suzue, K., T. Asai, T. Takeuchi, and S. Koyasu. 2003. In vivo role of IFN-γ produced by antigen-presenting cells in early host defense against intracellular pathogens. *Eur. J. Immunol.* 33: 2666–2675.
35. Geninat, G., S. Schenk, M. Skoberne, W. Goebel, and H. Hof. 2001. A novel approach of direct ex vivo epitope mapping identifies dominant and subdominant CD4 and CD8 T cell epitopes from *Listeria monocytogenes*. *J. Immunol.* 166: 1877–1884.
36. Wan, T., X. Zhou, G. Chen, H. An, T. Chen, W. Zhang, S. Liu, Y. Jiang, F. Yang, Y. Wu, and X. Cao. 2004. Novel heat shock protein Hsp70L1 activates dendritic cells and acts as a Th1 polarizing adjuvant. *Blood* 103: 1747–1754.
37. Wille-Reece, U., C. Y. Wu, B. J. Flynn, R. M. Kedl, and R. A. Seder. 2005. Immunization with HIV-1 Gag protein conjugated to a TLR7/8 agonist results in the generation of HIV-1 Gag-specific Th1 and $CD8^+$ T cell responses. *J. Immunol.* 174: 7676–7683.
38. Becker, P. D., S. Fiorentini, C. Link, G. Tosti, T. Ebensen, A. Caruso, and C. A. Guzman. 2006. The HIV-1 matrix protein p17 can be efficiently delivered by intranasal route in mice using the TLR 2/6 agonist MALP-2 as mucosal adjuvant. *Vaccine* 24: 5269–5276.
39. Lizee, G., G. Basha, J. Tiong, J. P. Julien, M. Tian, K. E. Biron, and W. A. Jefferies. 2003. Control of dendritic cell cross-presentation by the major histocompatibility complex class I cytoplasmic domain. *Nat. Immunol.* 4: 1065–1073.
40. Fujii, S., K. Liu, C. Smith, A. J. Bonito, and R. M. Steinman. 2004. The linkage of innate to adaptive immunity via maturing dendritic cells in vivo requires CD40 ligation in addition to antigen presentation and CD80/86 costimulation. *J. Exp. Med.* 199: 1607–1618.
41. Manickasingham, S. P., A. D. Edwards, O. Schulz, and C. Reis e Sousa. 2003. The ability of murine dendritic cell subsets to direct T helper cell differentiation is dependent on microbial signals. *Eur. J. Immunol.* 33: 101–107.
42. Den Haan, J. M., S. M. Lehar, and M. J. Bevan. 2000. $CD8^+$ but not $CD8^-$ dendritic cells cross-prime cytotoxic T cells in vivo. *J. Exp. Med.* 192: 1685–1696.
43. Maldonado-Lopez, R., T. De Smedt, P. Michel, J. Godfroid, B. Pajak, C. Heirman, K. Thielemans, O. Leo, J. Urbaim, and M. Moser. 1999. $CD8\alpha^+$ and $CD8\alpha^-$ subclasses of dendritic cells direct the development of distinct T helper cells in vivo. *J. Exp. Med.* 189: 587–592.